

# Adaptive Event-Triggered Synchronization of Reaction–Diffusion Neural Networks

Ruimei Zhang<sup>1</sup>, Deqiang Zeng<sup>2</sup>, Ju H. Park<sup>3</sup>, *Senior Member, IEEE*, Yajuan Liu<sup>4</sup>,  
and Xiangpeng Xie<sup>5</sup>, *Member, IEEE*

**Abstract**—This article focuses on the design of an adaptive event-triggered sampled-data control (ETSDC) mechanism for synchronization of reaction–diffusion neural networks (RDNNs) with random time-varying delays. Different from the existing ETSDC schemes with predetermined constant thresholds, an adaptive ETSDC mechanism is proposed for RDNNs. The adaptive ETSDC mechanism can be promptly adaptively adjusted since the threshold function is based on the current sampled and latest transmitted signals. Thus, the adaptive ETSDC mechanism can effectively save communication resources for RDNNs. By taking the influence of uncertain factors, the random time-varying delays are considered, which belongs to two intervals in a probabilistic way. Then, by constructing an appropriate Lyapunov–Krasovskii functional (LKF), new synchronization criteria are derived for RDNNs. By solving a set of linear matrix inequalities (LMIs), the desired adaptive ETSDC gain is obtained. Finally, the merits of the adaptive ETSDC mechanism and the effectiveness of the proposed results are verified by one numerical example.

**Index Terms**—Adaptive event-triggered mechanism, random time-varying delays, reaction–diffusion neural networks (RDNNs), sampled-data control.

## I. INTRODUCTION

**B**ECAUSE of the superiorities in learning algorithms and estimating data, neural networks (NNs) have provoked the increasing interests of many researchers. In recent years,

Manuscript received February 11, 2020; revised June 9, 2020 and September 22, 2020; accepted September 24, 2020. Date of publication October 15, 2020; date of current version August 4, 2021. The work of Ruimei Zhang was supported by the National Natural Science Foundation of China under Grant 62003229. The work of Ju H. Park was supported by the National Research Foundation of Korea (NRF) Grant funded by the Korea Government (Ministry of Science and ICT) under Grant 2019R1A5A8080290. The work of Xiangpeng Xie was supported in part by the National Natural Science Foundation of China under Grant 62022044 and in part by the Jiangsu Natural Science Foundation for Distinguished Young Scholars under Grant BK20190039. (*Corresponding author: Ju H. Park.*)

Ruimei Zhang is with the College of Cybersecurity, Sichuan University, Chengdu 610065, China (e-mail: ruimeizhang163@163.com).

Deqiang Zeng is with the School of Mathematics Sciences, Sichuan Normal University, Chengdu 610066, China, and also with the Data Recovery Key Laboratory of Sichuan Province, Neijiang Normal University, Neijiang 641100, China (e-mail: zengdq22@163.com).

Ju H. Park is with the Department of Electrical Engineering, Yeungnam University, Gyeongsan 38541, South Korea (e-mail: jessie@ynu.ac.kr).

Yajuan Liu is with the School of Control and Computer Engineering, North China Electric Power University, Beijing 102206, China (e-mail: yajuan.liu.12@gmail.com).

Xiangpeng Xie is with the Institute of Advanced Technology, Nanjing University of Posts and Telecommunications, Nanjing 210003, China (e-mail: xiexp@njupt.edu.cn).

Color versions of one or more of the figures in this article are available online at <https://ieeexplore.ieee.org>.

Digital Object Identifier 10.1109/TNNLS.2020.3027284

NNs have been successfully applied to diverse areas including cryptography, decryption, stock market prediction, signal processing, and model identification [1]–[7]. As an extension of NNs, reaction–diffusion NNs (RDNNs) have attracted much attention since they have been successfully applied to secure communication, population control, and artificial locomotion [8]–[12]. For example, reaction–diffusion cellular NNs have been successfully applied to artificial locomotion [10]. In [11], RDNNs have been applied to image encryption. In [12], RDNNs can effectively describe the different population densities of species, which are useful for better protecting and controlling the population. By taking the influence of reaction and diffusion of neurons into account, RDNNs can be represented by partial differential equations (PDEs), in which the neuron states are dependent on both time and space. Compared with traditional NNs, RDNNs exhibit more complicated and unpredictable behaviors. Hence, it is of great importance to study the dynamical behaviors of RDNNs.

Up until now, various dynamical behaviors of RDNNs, such as passivity [13], stability [14], and synchronization [15], have been investigated. Since the surprising discovery of synchronization in chaotic systems [16], synchronization has aroused substantial attention. It is motivated by the fact that the synchronization is ubiquitous in real systems and has many important engineering applications, including mechatronic systems, power systems, and secure communication [16]–[18]. Meanwhile, due to congestions of signal transmission and the finite switching speeds of amplifiers, time delays [19] inevitably exist in RDNNs. However, time delays have a great influence on the dynamical behaviors of RDNNs since they may result in oscillation, poor performance, or even instability. Moreover, due to the influence of uncertain factors and the limitations of equipment, random time-varying delays are often existent in natural and artificial systems. For example, in a shipboard gun fire control system, missynchronization between samples of the actual position and the inertial sensor and radar data samples results in the random time-varying delays [20]. Because of the asynchronous time-division-multiplexed networks, randomly varying distributed delays have been considered for the flight control system [21]. Using the statistical technique, random time-varying delays have been taken into account for power systems [22]. In recent years, random time-varying delays have been widely studied for many systems [23]–[25]. Thus, it is necessary to introduce random time-varying delays to RDNNs, and the investigation of synchronization control of RDNNs with random time-varying delays is particularly important.

Up until now, many control approaches have been proposed for synchronization of RDNNs with time delays, which includes impulsive control [26], pinning impulsive control [27], adaptive control [28], and feedback control [29]. For instance, in [27], by pinning impulsive control, the exponential synchronization problem has been considered for RDNNs with time delays. In [28], the antisynchronization of RDNNs with time delays has been studied by distributed adaptive control. In [29], by state feedback control, the asymptotic synchronization has been investigated for Markovian RDNNs with time delays. With the rapid growing of digital and communication technologies, sampled-data control is in the spotlight [30]–[32]. Compared with the forenamed control schemes, sampled-data control shows more merits, such as high reliability, easy installation, and low control cost. Thus, based on sampled-data control, the synchronization of RDNNs with time delays has been extensively investigated, and many interesting results are available in the literature [33]–[35]. Notice that all the aforesaid sampled-data control schemes are based on a time-triggered mechanism, which is assumed that all the signals are transmitted to the controllers without any data processing. However, the communication resources and computing capability of RDNNs are often limited. Hence, it is very important to save communication resources for RDNNs.

Recently, wide attention has been drawn to event-triggered sampled-data control (ETSDC) [36]–[39], where the sampled signals are not transmitted only if a predetermined threshold condition is violated. Thus, ETSDC can effectively reduce the number of transmission signals. Nowadays, adaptive event-triggered control has fascinated considerable research interests [40]–[43]. For example, in [40], an adaptive event-triggered mechanism with continuous control input signals has been considered for multiagent systems, which needs to test the triggered condition continuously. In [41], an adaptive ETSDC method has been proposed for networked control systems, where the threshold is a time-dependent continuous function. Similar scheme is adopted in [42]. However, the adaptive ETSDC schemes in [41] and [42] may not be appropriate since only sampled signals can be input the scheme. In [43], a new adaptive ETSDC mechanism has been given for network-based power systems, where the threshold function is dependent on the discrete sampled signals. Notice that the scheme in [43] is based on the past and latest transmission signals, which may not update the threshold promptly. Thus, how to improve the existing adaptive ETSDC mechanism is still challenging. These issues motivate this work.

The objective of this study is to develop a novel adaptive ETSDC mechanism for the synchronization of RDNNs with time delays. The main contributions are as follows.

- 1) An improved adaptive ETSDC mechanism is proposed for RDNNs for the first time. The adaptive ETSDC mechanism is based on the current sampled and latest transmitted signals, which can be promptly adaptively adjusted and effectively save the communication resources for RDNNs.

- 2) Taking the influence of uncertain factors, the random time-varying delays are considered for RDNNs, which make the derived results more applicable.

## II. PROBLEM FORMULATION AND PRELIMINARIES

### A. Notations

Let  $I_n$  denote the  $n \times n$  identity matrix,  $0_n$  and  $0_{n,m}$  the  $n \times n$  and  $n \times m$  zero matrices,  $\mathfrak{R}^n$  the  $n$ -dimensional Euclidean space, and  $\mathfrak{R}^{n \times n}$  the set of all  $n \times n$  real matrices.  $\text{diag}\{\cdots\}$  and  $\text{col}\{\cdots\}$  mean a block-diagonal matrix and a column vector, respectively.  $\lambda_{\min}(\cdot)$  stands for the minimum eigenvalue of a real symmetric matrix.  $\mathcal{E}\{\cdot\}$  represents the mathematical expectation with respect to the given probability measure  $\mathbb{P}$ .  $\text{Sym}\{\mathcal{H}\} = \mathcal{H} + \mathcal{H}^T$ .  $C([-d_2, 0] \times \Omega, \mathfrak{R}^n)$  means all continuous functions from  $[-d_2, 0] \times \Omega$  to  $\mathfrak{R}^n$ . For  $\psi \in C([-d_2, 0] \times \Omega, \mathfrak{R}^n)$ , the norm is defined by  $\|\psi(s, x)\| = \sup_{-d_2 \leq s \leq 0} \{(\int_{\Omega} \psi^T(s, x) \psi(s, x) dx)^{(1/2)}\}$ . For the vector  $\varpi(t, x) \in \mathfrak{R}^n$ , let  $\|\varpi(t, x)\|_{L^2} = (\int_{\Omega} \varpi^T(t, x) \varpi(t, x) dx)^{(1/2)}$ .

### B. Problem Formulation

Consider the following RDNNs with a random time-varying delay:

$$\begin{aligned} \frac{\partial \varpi(t, x)}{\partial t} &= \sum_{l=1}^m \frac{\partial}{\partial x_l} \left( A_l \frac{\partial \varpi(t, x)}{\partial x_l} \right) - \mathcal{C} \varpi(t, x) \\ &\quad + \mathcal{W}_1 g(\varpi(t, x)) + \mathcal{W}_2 g(\varpi(t - d(t), x)) \\ &\quad + J, \quad (t, x) \in [t_0^*, +\infty) \times \Omega \end{aligned} \quad (1)$$

$$\varpi(t, x) = 0, \quad (t, x) \in [t_0^* - d_2, +\infty) \times \partial \Omega \quad (2)$$

$$\varpi(s + t_0^*, x) = \psi_1(s, x) \in C([-d_2, 0] \times \Omega, \mathfrak{R}^n) \quad (3)$$

where  $l = 1, 2, \dots, m$ , and  $x = \text{col}\{x_1, x_2, \dots, x_m\} \in \Omega$ .  $\Omega \triangleq \{x | \underline{\varrho}_l \leq x_l \leq \bar{\varrho}_l\}$  with  $\partial \Omega$  being its boundary, and  $\underline{\varrho}_l$  and  $\bar{\varrho}_l$  are constants.  $A_l = \text{diag}\{a_{l1}, a_{l2}, \dots, a_{ln}\}$ , in which  $a_{li} > 0$  ( $i = 1, 2, \dots, n$ ) stands for the transmission diffusion coefficient.  $\mathcal{C} = \text{diag}\{c_1, c_2, \dots, c_n\}$  with  $c_i > 0$  ( $i = 1, 2, \dots, n$ ).  $\mathcal{W}_1 \in \mathfrak{R}^{n \times n}$  and  $\mathcal{W}_2 \in \mathfrak{R}^{n \times n}$  are the nondelayed and delayed connection weight matrices, respectively.  $\varpi(t, x) = \text{col}\{\varpi_1(t, x), \varpi_2(t, x), \dots, \varpi_n(t, x)\} \in \mathfrak{R}^n$  is the state vector at time  $t$  and in space  $x$ .  $g(\varpi(\cdot, x)) = \text{col}\{g_1(\varpi_1(\cdot, x)), g_2(\varpi_2(\cdot, x)), \dots, g_n(\varpi_n(\cdot, x))\} \in \mathfrak{R}^n$  is the neuron activation function.  $J \in \mathfrak{R}^n$  is an external input vector.  $d(t)$  is the random time-varying delay being in  $[0, d_1]$  or  $(d_1, d_2]$  with

$$\mathbb{P}\{d(t) \in [0, d_1]\} = \gamma, \quad \mathbb{P}\{d(t) \in (d_1, d_2]\} = 1 - \gamma \quad (4)$$

where  $0 \leq d_1 \leq d_2$ ,  $0 \leq \gamma \leq 1$ , and  $d_1$  and  $d_2$  are constants. Equations (2) and (3) are, respectively, the Dirichlet boundary condition and the initial condition.

Define stochastic variable  $\beta(t) = \begin{cases} 1, & d(t) \in [0, d_1] \\ 0, & d(t) \in (d_1, d_2]. \end{cases}$  We find

$$\begin{aligned} \mathbb{P}\{\beta(t) = 1\} &= \mathbb{P}\{d(t) \in [0, d_1]\} = \gamma \\ \mathbb{P}\{\beta(t) = 0\} &= \mathbb{P}\{d(t) \in (d_1, d_2]\} = 1 - \gamma. \end{aligned} \quad (5)$$

Let the time-varying delays  $d_i(t)$  ( $i = 1, 2$ ) satisfy  $d(t) = \begin{cases} d_1(t), & d(t) \in [0, d_1] \\ d_2(t), & d(t) \in (d_1, d_2], \end{cases}$  and  $\dot{d}_i(t) \leq \mu_i$  ( $i = 1, 2$ ). Then, RDNN (1) can be rewritten as

$$\begin{aligned} \frac{\partial \varpi(t, x)}{\partial t} &= \sum_{l=1}^m \frac{\partial}{\partial x_l} \left( \mathcal{A}_l \frac{\partial \varpi(t, x)}{\partial x_l} \right) - \mathcal{C} \varpi(t, x) \\ &\quad + \mathcal{W}_1 g(\varpi(t, x)) + \beta(t) \mathcal{W}_2 g(\varpi(t - d_1(t), x)) \\ &\quad + (1 - \beta(t)) \mathcal{W}_2 g(\varpi(t - d_2(t), x)) + J. \end{aligned} \quad (6)$$

Viewing system (6) as the drive system, the corresponding controlled response system is described as

$$\begin{aligned} \frac{\partial z(t, x)}{\partial t} &= \sum_{l=1}^m \frac{\partial}{\partial x_l} \left( \mathcal{A}_l \frac{\partial z(t, x)}{\partial x_l} \right) - \mathcal{C} z(t, x) \\ &\quad + \mathcal{W}_1 g(z(t, x)) + \beta(t) \mathcal{W}_2 g(z(t - d_1(t), x)) \\ &\quad + (1 - \beta(t)) \mathcal{W}_2 g(z(t - d_2(t), x)) \\ &\quad + \mathcal{U}(t, x) + J, \quad (t, x) \in [t_0^{**}, +\infty) \times \Omega \end{aligned} \quad (7)$$

$$z(t, x) = 0, \quad (t, x) \in [t_0^{**} - d_2, +\infty) \times \partial\Omega \quad (8)$$

$$z(s + t_0^{**}, x) = \psi_2(s, x) \in C([-d_2, 0] \times \Omega, \mathfrak{R}^n) \quad (9)$$

where  $\mathcal{U}(t, x) \in \mathfrak{R}^n$  is the control signal.

Let the error signal  $\vartheta(t, x) = z(t, x) - \varpi(t, x) = \text{col}\{\vartheta_1(t, x), \vartheta_2(t, x), \dots, \vartheta_n(t, x)\} \in \mathfrak{R}^n$ . From (6) and (7), we have the error system as

$$\begin{aligned} \frac{\partial \vartheta(t, x)}{\partial t} &= \sum_{l=1}^m \frac{\partial}{\partial x_l} \left( \mathcal{A}_l \frac{\partial \vartheta(t, x)}{\partial x_l} \right) - \mathcal{C} \vartheta(t, x) \\ &\quad + \mathcal{W}_1 f(\vartheta(t, x)) + \beta(t) \mathcal{W}_2 f(\vartheta(t - d_1(t), x)) \\ &\quad + (1 - \beta(t)) \mathcal{W}_2 f(\vartheta(t - d_2(t), x)) \\ &\quad + \mathcal{U}(t, x), \quad (t, x) \in [\tilde{t}_0, +\infty) \times \Omega \end{aligned} \quad (10)$$

$$\vartheta(t, x) = 0, \quad (t, x) \in [\tilde{t}_0 - d_2, +\infty) \times \partial\Omega \quad (11)$$

$$\vartheta(s + \tilde{t}_0, x) = \psi(s, x) \in C([-d_2, 0] \times \Omega, \mathfrak{R}^n) \quad (12)$$

where  $f(\vartheta(t, x)) = g(z(t, x)) - g(\varpi(t, x))$  and  $\tilde{t}_0 = \max\{t_0^*, t_0^{**}\}$ .

In order to save the limited communication resources of RDNNs, an adaptive event-triggered generator with aperiodic sampled-data signals will be introduced, in which the threshold function can be promptly adaptively adjusted based on the current sampled and latest transmitted signals.

Let the input signals be generated by a zero-order-hold (ZOH) function with the holding times  $0 = t_0 < t_1 < t_2 < \dots < t_k < \dots$ . The nonuniform sampling interval  $h_k$  satisfies the following condition:

$$h_k = t_{k+1} - t_k \leq \tilde{h}$$

where  $\tilde{h} > 0$  is a constant.

Then, we propose the following adaptive event-triggered communication mechanism:

$$\begin{aligned} i_p &= t_{\sigma_{p-1}}, \quad p \in \mathbb{N} \\ \sigma_{p-1} &= \begin{cases} 0, & p = 0 \\ \sum_{k=0}^{p-1} \tau_k, & p \in \mathbb{N}^+ \end{cases} \end{aligned}$$

$$\begin{aligned} \tau_k &= \inf \left\{ \tau \mid \delta(t_{\sigma_{k-1}+\tau}) \|\mathcal{B}_1^{\frac{1}{2}} \vartheta(t_{\sigma_{k-1}}, x)\|_{L^2}^2 \right. \\ &\quad \left. < \|\mathcal{B}_2^{\frac{1}{2}} e(t_{\sigma_{k-1}+\tau}, x)\|_{L^2}^2, \quad \tau \in \mathbb{N}^+ \right\}, \quad k \in \mathbb{N} \end{aligned} \quad (13)$$

to determine whether the newly sampled signal should be transmitted, where  $\mathcal{B}_1 > 0 \in \mathfrak{R}^{n \times n}$  and  $\mathcal{B}_2 > 0 \in \mathfrak{R}^{n \times n}$  are weighting matrices, and  $e(t_{\sigma_{k-1}+\tau}, x)$  is defined as  $e(t_{\sigma_{k-1}+\tau}, x) \triangleq \vartheta(t_{\sigma_{k-1}+\tau}, x) - \vartheta(t_{\sigma_{k-1}}, x)$ , which is the state error between the current instant and latest transmitted instant. The event-triggered transmission sequence is described by  $\mathfrak{I}_1 = \{i_0, i_1, i_2, \dots, i_p, \dots\} \subseteq \mathfrak{I}_2 = \{t_0, t_1, t_2, \dots, t_k, \dots\}$ .

It is noted that the threshold  $\delta(t_{\sigma_{k-1}+\tau})$  in (13) is time-varying, which can be adaptively adjusted based on the current sampled and latest transmitted signals, that is, for  $\tau \in \mathbb{N}^+$

$$\delta(t_{\sigma_{k-1}+\tau}) = (1 + \alpha(t_{\sigma_{k-1}+\tau})) \delta(t_{\sigma_{k-1}+\tau-1}) \quad (14)$$

where

$$\begin{aligned} \alpha(t_{\sigma_{k-1}+\tau}) &= \begin{cases} \frac{\delta_0}{\theta} - 1, & \|\vartheta(t_{\sigma_{k-1}+\tau}, x)\|_{L^2} \geq \|\vartheta(t_{\sigma_{k-1}}, x)\|_{L^2} \\ \theta \frac{\|\vartheta(t_{\sigma_{k-1}}, x)\|_{L^2} - \|\vartheta(t_{\sigma_{k-1}+\tau}, x)\|_{L^2}}{\|\vartheta(t_{\sigma_{k-1}}, x)\|_{L^2}}, & \text{otherwise} \end{cases} \end{aligned}$$

where  $\theta$  is a positive scalar.

*Proposition 1:* Give the initial value of  $\delta(t)$  as  $\delta(t_0) = \delta_0$ . For  $\forall \tau \in \mathbb{N}^+, k \in \mathbb{N}$ , the inequalities

$$\delta(t_{\sigma_{k-1}+\tau}) \geq \delta_0$$

hold.

*Proof:* From  $\delta(t_{\sigma_{k-1}+\tau}) = (1 + \alpha(t_{\sigma_{k-1}+\tau})) \delta(t_{\sigma_{k-1}+\tau-1})$  and the definition of  $\alpha(t_{\sigma_{k-1}+\tau})$  in (14), one gets

$$\delta(t_1) = \delta_0 \quad \text{or} \quad \delta(t_1) > \delta_0$$

which implies that  $\delta(t_1) \geq \delta_0$ . To continue this process, one can derive for  $\forall \tau \in \mathbb{N}^+, k \in \mathbb{N}$

$$\delta(t_{\sigma_{k-1}+\tau}) \geq \delta_0.$$

This completes the proof.  $\blacksquare$

*Remark 1:* It is worth mentioning that the adaptive event-triggered communication mechanism (13) is newly designed for RDNNs. By adaptively adjusting the threshold  $\delta(t_{\sigma_{k-1}+\tau})$ , the mechanism (13) can effectively reduce the number of transmission signals. When  $\|\vartheta(t_{\sigma_{k-1}+\tau}, x)\|_{L^2} \geq \|\vartheta(t_{\sigma_{k-1}}, x)\|_{L^2}$ , one can derive  $\delta(t_{\sigma_{k-1}+\tau}) = \delta_0$ , which implies that the mechanism (13) uses the smaller threshold  $\delta_0$  to produce a higher transmission frequency to strengthen the control. When  $\|\vartheta(t_{\sigma_{k-1}+\tau}, x)\|_{L^2} < \|\vartheta(t_{\sigma_{k-1}}, x)\|_{L^2}$ , one finds  $\delta(t_{\sigma_{k-1}+\tau}) > \delta(t_{\sigma_{k-1}+\tau-1})$ , which implies that the mechanism (13) uses the larger value of  $\delta(t_{\sigma_{k-1}+\tau})$  to produce a lower transmission frequency to attenuate the control.

*Remark 2:* In [40], the adaptive event-triggered scheme is designed with continuous input signals, which requires to test the trigger condition continuously. In [41] and [42], a continuous time-dependent threshold function is introduced to the adaptive event-triggered schemes. However, these schemes



$$\begin{aligned}
&= \text{Sym}\{\mathcal{I}_1^T \mathcal{P} \mathcal{I}_4\} + \gamma [\mathcal{I}_1^T, \mathcal{I}_3^T] \mathcal{Q}_1 [\mathcal{I}_1^T, \mathcal{I}_3^T]^T \\
&\quad - \gamma (1 - \mu_1) [\mathcal{I}_6^T, \mathcal{I}_8^T] \mathcal{Q}_1 [\mathcal{I}_6^T, \mathcal{I}_8^T]^T \\
&\quad + (1 - \gamma) [\mathcal{I}_1^T, \mathcal{I}_3^T] \mathcal{Q}_2 [\mathcal{I}_1^T, \mathcal{I}_3^T]^T \\
&\quad - (1 - \gamma)(1 - \mu_2) [\mathcal{I}_7^T, \mathcal{I}_9^T] \mathcal{Q}_2 [\mathcal{I}_7^T, \mathcal{I}_9^T]^T \\
\Xi_4(\rho; h_{\sigma_{p-1+j}}, h(t)) &= (h_{\sigma_{p-1+j}} - h(t)) \text{Sym}\{(\mathcal{I}_1 - \mathcal{I}_2)^T \mathcal{T} \mathcal{I}_4\} \\
&\quad - (\mathcal{I}_1 - \mathcal{I}_2)^T \mathcal{T} (\mathcal{I}_1 - \mathcal{I}_2) \\
&\quad + (h_{\sigma_{p-1+j}} - h(t)) \mathcal{I}_4^T \mathcal{R} \mathcal{I}_4 \\
&\quad - \text{Sym}\{(\mathcal{I}_1 - \mathcal{I}_2)^T \mathcal{H}_1 [\mathcal{I}_1^T, \mathcal{I}_2^T]^T\} \\
&\quad + \rho h(t) [\mathcal{I}_1^T, \mathcal{I}_2^T] \mathcal{H}_1^T \mathcal{R}^{-1} \mathcal{H}_1 [\mathcal{I}_1^T, \mathcal{I}_2^T]^T \\
&\quad - 3 \text{Sym}\{(\mathcal{I}_1 + \mathcal{I}_2 - 2\mathcal{I}_5)^T \mathcal{H}_2 [\mathcal{I}_1^T, \mathcal{I}_2^T, \mathcal{I}_5^T]^T\} \\
&\quad + 3 \rho h(t) [\mathcal{I}_1^T, \mathcal{I}_2^T, \mathcal{I}_5^T] \mathcal{H}_2^T \mathcal{R}^{-1} \mathcal{H}_2 [\mathcal{I}_1^T, \mathcal{I}_2^T, \mathcal{I}_5^T]^T \\
\Xi_5(\rho; h_{\sigma_{p-1+j}}, h(t)) &= \text{Sym}\{(\mathcal{I}_4^T + \kappa \mathcal{I}_1^T) \mathcal{S} (-\mathcal{I}_4 - \mathcal{C} \mathcal{I}_1 + \mathcal{W}_1 \mathcal{I}_3 + \gamma \mathcal{W}_2 \mathcal{I}_8 \\
&\quad + (1 - \gamma) \mathcal{W}_2 \mathcal{I}_9)\} - 2\kappa \sum_{l=1}^m \frac{\pi^2}{(\underline{q}_l - \underline{q}_j)^2} \mathcal{I}_1^T \mathcal{S} \mathcal{A}_l \mathcal{I}_1 \\
&\quad + \text{Sym}\{(\mathcal{I}_4^T + \kappa \mathcal{I}_1^T) \mathcal{S} \mathcal{K} (\mathcal{I}_2 - \mathcal{I}_{10})\}.
\end{aligned}$$

*Proof:* Choose an LKF candidate for system (17) as

$$\mathcal{V}(t) = \sum_{i=1}^5 \mathcal{V}_i(t), \quad t \in F_j \quad (23)$$

where

$$\begin{aligned}
\mathcal{V}_1(t) &= \int_{\Omega} \vartheta^T(t, x) \mathcal{P} \vartheta(t, x) dx \\
\mathcal{V}_2(t) &= \gamma \int_{\Omega} \int_{t-d_1(t)}^t \xi_1^T(s, x) \mathcal{Q}_1 \xi_1(s, x) ds dx \\
&\quad + (1 - \gamma) \int_{\Omega} \int_{t-d_2(t)}^t \xi_1^T(s, x) \mathcal{Q}_2 \xi_1(s, x) ds dx \\
\mathcal{V}_3(t) &= (h_{\sigma_{p-1+j}} - h(t)) \int_{\Omega} \xi_2^T(t, x) \mathcal{T} \xi_2(t, x) dx \\
\mathcal{V}_4(t) &= \int_{\Omega} \sum_{l=1}^m \frac{\partial \vartheta^T(t, x)}{\partial x_l} \mathcal{S} \mathcal{A}_l \frac{\partial \vartheta(t, x)}{\partial x_l} dx \\
\mathcal{V}_5(t) &= (h_{\sigma_{p-1+j}} - h(t)) \\
&\quad \cdot \int_{\Omega} \int_{t_{\sigma_{p-1+j}}}^t \frac{\partial \vartheta^T(s, x)}{\partial s} \mathcal{R} \frac{\partial \vartheta(s, x)}{\partial s} ds dx
\end{aligned}$$

with  $\xi_1(t, x) = \text{col}\{\vartheta(t, x), f(\vartheta(t, x))\}$  and  $\xi_2(t, x) = \vartheta(t, x) - \vartheta(t - h(t), x)$ .

It is noted that  $\lim_{t \rightarrow t_{\sigma_{p-1+j}}} \mathcal{V}_i(t) = 0$  ( $i = 3, 5$ ), which means that  $\mathcal{V}_i(t)$  ( $i = 3, 5$ ) vanish before and after  $t_{\sigma_{p-1+j}}$ . Thus,  $\mathcal{V}(t)$  is continuous in time. In the meantime, one finds that

$$\mathcal{V}(t_{\sigma_{p-1+j}}) = \sum_{i=1,2,4} \mathcal{V}_i(t_{\sigma_{p-1+j}}) \geq 0. \quad (24)$$

Let  $\mathcal{L}$  be the infinitesimal operator [47] along error system (17). Then,  $\mathcal{L}\{\mathcal{V}(t)\}$  is calculated as

$$\mathcal{L}\{\mathcal{V}(t)\} = \sum_{i=1}^5 \mathcal{L}\{\mathcal{V}_i(t)\} \quad (25)$$

where  $\mathcal{L}\{\mathcal{V}_i(t)\}$  ( $i = 1, 2, \dots, 5$ ) are listed as

$$\mathcal{L}\{\mathcal{V}_1(t)\} = \mathcal{L} \left\{ 2 \int_{\Omega} \vartheta^T(t, x) \mathcal{P} \frac{\partial \vartheta(t, x)}{\partial t} dx \right\} \quad (26)$$

$$\begin{aligned}
\mathcal{L}\{\mathcal{V}_2(t)\} &\leq \mathcal{L} \left\{ \gamma \int_{\Omega} \xi_1^T(t, x) \mathcal{Q}_1 \xi_1(t, x) dx - \gamma (1 - \mu_1) \right. \\
&\quad \cdot \int_{\Omega} \xi_1^T(t - d_1(t), x) \mathcal{Q}_1 \xi_1(t - d_1(t), x) dx \\
&\quad + (1 - \gamma) \int_{\Omega} \xi_1^T(t, x) \mathcal{Q}_2 \xi_1(t, x) dx - (1 - \gamma)(1 - \mu_2) \\
&\quad \cdot \left. \int_{\Omega} \xi_1^T(t - d_2(t), x) \mathcal{Q}_2 \xi_1(t - d_2(t), x) dx \right\} \quad (27)
\end{aligned}$$

$$\begin{aligned}
\mathcal{L}\{\mathcal{V}_3(t)\} &= \mathcal{L} \left\{ 2(h_{\sigma_{p-1+j}} - h(t)) \int_{\Omega} \xi_2^T(t, x) \mathcal{T} \frac{\partial \vartheta(t, x)}{\partial t} dx \right. \\
&\quad \left. - \int_{\Omega} \xi_2^T(t, x) \mathcal{T} \xi_2(t, x) dx \right\} \quad (28)
\end{aligned}$$

$$\begin{aligned}
\mathcal{L}\{\mathcal{V}_4(t)\} &= \mathcal{L} \left\{ 2 \int_{\Omega} \sum_{l=1}^m \frac{\partial^2 \vartheta^T(t, x)}{\partial x_l \partial t} \mathcal{S} \mathcal{A}_l \frac{\partial \vartheta(t, x)}{\partial x_l} dx \right\} \quad (29)
\end{aligned}$$

$$\begin{aligned}
\mathcal{L}\{\mathcal{V}_5(t)\} &= \mathcal{L} \left\{ - \int_{\Omega} \int_{t_{\sigma_{p-1+j}}}^t \frac{\partial \vartheta^T(s, x)}{\partial s} \mathcal{R} \frac{\partial \vartheta(s, x)}{\partial s} ds dx \right. \\
&\quad \left. + (h_{\sigma_{p-1+j}} - h(t)) \int_{\Omega} \frac{\partial \vartheta^T(t, x)}{\partial t} \mathcal{R} \frac{\partial \vartheta(t, x)}{\partial t} dx \right\}. \quad (30)
\end{aligned}$$

When the current sampled signal is not transmitted to the controller, from (13) and Proposition 1, one gets the following inequality:

$$\begin{aligned}
\delta_0 \|\mathcal{B}_1^{\frac{1}{2}}(\vartheta(t - h(t), x) - e(t - h(t), x))\|_{L^2}^2 \\
- \|\mathcal{B}_2^{\frac{1}{2}} e(t - h(t), x)\|_{L^2}^2 \geq 0 \quad (31)
\end{aligned}$$

which is equivalent to

$$\begin{aligned}
\delta_0 \int_{\Omega} (\vartheta(t - h(t), x) - e(t - h(t), x))^T \mathcal{B}_1 \\
\cdot (\vartheta(t - h(t), x) - e(t - h(t), x)) dx \\
- \int_{\Omega} e^T(t - h(t), x) \mathcal{B}_2 e(t - h(t), x) dx \geq 0. \quad (32)
\end{aligned}$$

According to Lemma 1, from (30), we have

$$\begin{aligned}
- \int_{\Omega} \int_{t_{\sigma_{p-1+j}}}^t \frac{\partial \vartheta^T(s, x)}{\partial s} \mathcal{R} \frac{\partial \vartheta(s, x)}{\partial s} ds dx \\
\leq - \frac{1}{h(t)} \int_{\Omega} \xi_2^T(t, x) \mathcal{R} \xi_2(t, x) dx \\
- \frac{3}{h(t)} \int_{\Omega} \xi_4^T(t, x) \mathcal{R} \xi_4(t, x) dx \quad (33)
\end{aligned}$$

where  $\xi_4(t, x) = \vartheta(t, x) + \vartheta(t - h(t), x) - 2\xi_3(t, x)$ .

For any matrices  $\mathcal{H}_1 \in \mathfrak{N}^{n \times 2n}$  and  $\mathcal{H}_2 \in \mathfrak{N}^{n \times 3n}$ , we find that

$$\int_{\Omega} \frac{1}{h(t)} (\mathcal{R} \xi_2(t, x) - h(t) \mathcal{H}_1 \xi_5(t, x))^T \mathcal{R}^{-1}$$

$$\begin{aligned} & \cdot (\mathcal{R}\xi_2(t, x) - h(t)\mathcal{H}_1\xi_5(t, x))dx \geq 0 \quad (34) \\ & \int_{\Omega} \frac{1}{h(t)} (\mathcal{R}\xi_4(t, x) - h(t)\mathcal{H}_2\xi_6(t, x))^T \mathcal{R}^{-1} \\ & \cdot (\mathcal{R}\xi_4(t, x) - h(t)\mathcal{H}_2\xi_6(t, x))dx \geq 0 \quad (35) \end{aligned}$$

from which one can obtain

$$\begin{aligned} & -\frac{1}{h(t)} \int_{\Omega} \xi_2^T(t, x) \mathcal{R}\xi_2(t, x) dx \\ & \leq -2 \int_{\Omega} \xi_2^T(t, x) \mathcal{H}_1\xi_5(t, x) dx \\ & \quad + h(t) \int_{\Omega} \xi_5^T(t, x) \mathcal{H}_1^T \mathcal{R}^{-1} \mathcal{H}_1\xi_5(t, x) dx \quad (36) \\ & -\frac{3}{h(t)} \int_{\Omega} \xi_4^T(t, x) \mathcal{R}\xi_4(t, x) dx \\ & \leq -6 \int_{\Omega} \xi_4^T(t, x) \mathcal{H}_2\xi_6(t, x) dx \\ & \quad + 3h(t) \int_{\Omega} \xi_6^T(t, x) \mathcal{H}_2^T \mathcal{R}^{-1} \mathcal{H}_2\xi_6(t, x) dx \quad (37) \end{aligned}$$

where  $\xi_5(t, x) = \text{col}\{\vartheta(t, x), \vartheta(t - h(t), x)\}$  and  $\xi_6(t, x) = \text{col}\{\vartheta(t, x), \vartheta(t - h(t), x), \xi_3(t, x)\}$ .

From the error system (17), one has the following zero equality:

$$\begin{aligned} 0 = \mathcal{E} \left\{ 2 \int_{\Omega} \left[ \frac{\partial \vartheta(t, x)}{\partial t} + \kappa \vartheta(t, x) \right]^T \mathcal{S} \right. \\ \times \left[ -\frac{\partial \vartheta(t, x)}{\partial t} + \sum_{l=1}^m \mathcal{A}_l \frac{\partial^2 \vartheta(t, x)}{\partial x_l^2} - \mathcal{C}\vartheta(t, x) \right. \\ \left. + \mathcal{W}_1 f(\vartheta(t, x)) + \gamma \mathcal{W}_2 f(\vartheta(t - d_1(t), x)) \right. \\ \left. + (1 - \gamma) \mathcal{W}_2 f(\vartheta(t - d_2(t), x)) \right. \\ \left. + \mathcal{K}(\vartheta(t - h(t), x) - e(t - h(t), x)) \right] dx \Big\}. \quad (38) \end{aligned}$$

Based on the Green formula, the Dirichlet boundary condition (18), and (38), we can find that

$$\begin{aligned} & 2 \int_{\Omega} \frac{\partial \vartheta^T(t, x)}{\partial t} \mathcal{S} \sum_{l=1}^m \mathcal{A}_l \frac{\partial \vartheta^2(t, x)}{\partial x_l^2} dx \\ & = 2 \int_{\partial\Omega} \sum_{l=1}^m \frac{\partial \vartheta^T(t, x)}{\partial t} \mathcal{S} \mathcal{A}_l \frac{\partial \vartheta(t, x)}{\partial x_l} dx \\ & \quad - 2 \int_{\Omega} \sum_{l=1}^m \frac{\partial^2 \vartheta^T(t, x)}{\partial x_l \partial t} \mathcal{S} \mathcal{A}_l \frac{\partial \vartheta(t, x)}{\partial x_l} dx \\ & = -2 \int_{\Omega} \sum_{l=1}^m \frac{\partial^2 \vartheta^T(t, x)}{\partial x_l \partial t} \mathcal{S} \mathcal{A}_l \frac{\partial \vartheta(t, x)}{\partial x_l} dx. \quad (39) \end{aligned}$$

Similarly, one derives from Lemma 2 that

$$\begin{aligned} & 2\kappa \int_{\Omega} \vartheta^T(t, x) \mathcal{S} \sum_{l=1}^m \mathcal{A}_l \frac{\partial \vartheta^2(t, x)}{\partial x_l^2} dx \\ & = -2\kappa \int_{\Omega} \sum_{l=1}^m \frac{\partial \vartheta^T(t, x)}{\partial x_l} \mathcal{S} \mathcal{A}_l \frac{\partial \vartheta(t, x)}{\partial x_l} dx \\ & \leq -2\kappa \int_{\Omega} \sum_{l=1}^m \frac{\pi^2}{(\underline{q}_l - \bar{q}_l)^2} \vartheta^T(t, x) \mathcal{S} \mathcal{A}_l \vartheta(t, x) dx. \quad (40) \end{aligned}$$

According to Assumption 1, for any diagonal matrices  $\mathcal{D}_i > 0 \in \mathfrak{R}^{n \times n}$  ( $i = 1, 2, 3$ ), one obtains

$$\begin{aligned} & \int_{\Omega} 2(f(\vartheta(t, x)) - \mathcal{F}^{-}\vartheta(t, x))^T \mathcal{D}_1 \\ & \cdot (\mathcal{F}^{+}\vartheta(t, x) - f(\vartheta(t, x))) dx \geq 0 \\ & \int_{\Omega} 2(f(\vartheta(t - d_1(t), x)) - \mathcal{F}^{-}\vartheta(t - d_1(t), x))^T \mathcal{D}_2 \\ & \cdot (\mathcal{F}^{+}\vartheta(t - d_1(t), x) - f(\vartheta(t - d_1(t), x))) dx \geq 0 \\ & \int_{\Omega} 2(f(\vartheta(t - d_2(t), x)) - \mathcal{F}^{-}\vartheta(t - d_2(t), x))^T \mathcal{D}_3 \\ & \cdot (\mathcal{F}^{+}\vartheta(t - d_2(t), x) - f(\vartheta(t - d_2(t), x))) dx \geq 0. \quad (41) \end{aligned}$$

Combining (25)–(41), for  $t \in F_j$ , we obtain

$$\begin{aligned} & \mathcal{E}\{\mathcal{L}\mathcal{V}(t)\} \\ & \leq \mathcal{E} \left\{ \int_{\Omega} \eta^T(t, x) \Xi(1; h_{\sigma_{p-1+j}}, h(t)) \eta(t, x) dx \right\} \\ & = \mathcal{E} \left\{ \int_{\Omega} \eta^T(t, x) \left[ \frac{h_{\sigma_{p-1+j}} - h(t)}{\tilde{h}} \Xi(1; \tilde{h}, 0) + \frac{h(t)}{\tilde{h}} \right. \right. \\ & \quad \left. \left. \times \Xi(1; \tilde{h}, \tilde{h}) + \frac{\tilde{h} - h_{\sigma_{p-1+j}}}{\tilde{h}} \Xi(1; 0, 0) \right] \eta(t, x) dx \right\}. \quad (42) \end{aligned}$$

Using the Schur complement to (22) and from (20)–(22) and (42), one finds that

$$\mathcal{E}\{\mathcal{L}\mathcal{V}(t)\} \leq 0, \quad t \in F_j \quad (43)$$

from which we derive

$$\begin{aligned} & \mathcal{E}\{\mathcal{L}\mathcal{V}(t)\} \leq -\varepsilon \mathcal{E} \left\{ \int_{\Omega} \eta^T(t, x) \eta(t, x) dx \right\} \\ & \leq -\varepsilon \mathcal{E}\{\|\vartheta(t, x)\|_{L_2}^2\}, \quad t \in F_j \quad (44) \end{aligned}$$

where  $\varepsilon = \min\{\lambda_{\min}(-\Xi(1; \tilde{h}, 0)), \lambda_{\min}(-\Xi(1; \tilde{h}, \tilde{h})), \lambda_{\min}(-\Xi(1; 0, 0))\}$ .

For  $\eta(t, x) \neq 0$ , we have from (24) and (43) that

$$\begin{aligned} & \mathcal{V}(t) > \mathcal{V}(t_{\sigma_{p-1+j+1}}^-) = \mathcal{V}(t_{\sigma_{p-1+j+1}}) > 0 \\ & t \in F_j, \quad j = 0, 1, 2, \dots, \tau_p - 1 \quad (45) \end{aligned}$$

which implies that  $\mathcal{V}(t)$  is positive definite.

By the Itô's formula, one gets

$$\mathcal{E}\{\mathcal{V}(t)\} - \mathcal{E}\{\mathcal{V}(\tilde{t}_0)\} = \mathcal{E} \left\{ \int_{\tilde{t}_0}^t \mathcal{L}\mathcal{V}(s) ds \right\}. \quad (46)$$

Then, from (23) and (44)–(46), there exists a scalar  $\iota > 0$  such that

$$\begin{aligned} & \iota \mathcal{E}\{\|\vartheta(t, x)\|_{L_2}^2\} \leq \mathcal{E}\{\mathcal{V}(t)\} \\ & = \mathcal{E}\{\mathcal{V}(\tilde{t}_0)\} + \mathcal{E} \left\{ \int_{\tilde{t}_0}^t \mathcal{L}\mathcal{V}(s) ds \right\} \\ & \leq \mathcal{E}\{\mathcal{V}(\tilde{t}_0)\} - \varepsilon \int_{\tilde{t}_0}^t \mathcal{E}\{\|\vartheta(s, x)\|_{L_2}^2\} ds. \quad (47) \end{aligned}$$

Thus, the error system (17) is asymptotically stable. This completes the proof.  $\blacksquare$

*Remark 4:* Based on the Lyapunov stability theory, it is crucial to choose an appropriate LKF for deriving stability criteria. In this article, (23) is chosen as the LKF.  $\mathcal{V}_1(t)$  is the basic term.  $\mathcal{V}_4(t)$  is constructed to counteract the reaction–diffusion term  $2 \int_{\Omega} ((\partial \vartheta^T(t, x))/\partial t) \mathcal{S} \sum_{l=1}^m \mathcal{A}_l ((\partial \vartheta^2(t, x))/\partial x_l^2) dx$  in (38). It is well known that delay information and sampling information is effective to reduce the conservatism of stability criteria. Thus,  $\mathcal{V}_2(t)$  is introduced to capture the information of the time delay  $d(t)$ .  $\mathcal{V}_3(t)$  and  $\mathcal{V}_5(t)$  are used to capture the information of sampling.

### B. Adaptive Event-Triggered Sampled-Data Controller Design

When the controller gain  $\mathcal{K}$  is not given, based on Theorem 1, the adaptive event-triggered sampled-data controller (16) is designed for synchronization of the RDNNs (1) and (7) as follows.

*Theorem 2:* For given scalars  $0 \leq \gamma \leq 1$ ,  $\mu_i$  ( $i = 1, 2$ ),  $\tilde{h} > 0$ ,  $\delta_0$ , and  $\kappa$ , the response RDNN (7) is asymptotically synchronized to the drive RDNN (1) if there exist matrices  $\mathcal{P} > 0 \in \mathfrak{R}^{n \times n}$ ,  $\mathcal{Q}_i > 0 \in \mathfrak{R}^{2n \times 2n}$  ( $i = 1, 2$ ),  $\mathcal{T} > 0 \in \mathfrak{R}^{n \times n}$ ,  $\mathcal{R} > 0 \in \mathfrak{R}^{n \times n}$ , and  $\mathcal{B}_i > 0 \in \mathfrak{R}^{n \times n}$  ( $i = 1, 2$ ), diagonal matrices  $\mathcal{D}_i > 0 \in \mathfrak{R}^{n \times n}$  ( $i = 1, 2, 3$ ), and any matrices  $\mathcal{S} \in \mathfrak{R}^{n \times n}$ ,  $\mathcal{H}_1 \in \mathfrak{R}^{n \times 2n}$ ,  $\mathcal{H}_2 \in \mathfrak{R}^{n \times 3n}$ , and  $\mathcal{K}^* \in \mathfrak{R}^{n \times n}$  satisfying  $\mathcal{S}\mathcal{A}_l \geq 0$  and

$$\Xi^*(0; 0, 0) < 0 \quad (48)$$

$$\Xi^*(0; \tilde{h}, 0) < 0 \quad (49)$$

$$\begin{bmatrix} \Xi^*(0; \tilde{h}, \tilde{h}) & \sqrt{\tilde{h}}[\mathcal{I}_1^T, \mathcal{I}_2^T]\mathcal{H}_1^T & \sqrt{3\tilde{h}}[\mathcal{I}_1^T, \mathcal{I}_2^T, \mathcal{I}_5^T]\mathcal{H}_2^T \\ * & -\mathcal{R} & 0 \\ * & * & -\mathcal{R} \end{bmatrix} < 0 \quad (50)$$

where  $\Xi^*(\rho; h_{\sigma_{p-1+j}}, h(t)) = \sum_{i=1}^4 \Xi_i(\rho; h_{\sigma_{p-1+j}}, h(t)) + \Xi_5^*(\rho; h_{\sigma_{p-1+j}}, h(t))$  with

$$\begin{aligned} \Xi_5^*(\rho; h_{\sigma_{p-1+j}}, h(t)) \\ = \text{Sym}\{(\mathcal{I}_4^T + \kappa\mathcal{I}_1^T)\mathcal{S}(-\mathcal{I}_4 - \mathcal{C}\mathcal{I}_1 + \mathcal{W}_1\mathcal{I}_3 + \gamma\mathcal{W}_2\mathcal{I}_8 \\ + (1 - \gamma)\mathcal{W}_2\mathcal{I}_9)\} - 2\kappa \sum_{l=1}^m \frac{\pi^2}{(\bar{\varrho}_l - \underline{\varrho}_l)^2} \mathcal{I}_1^T \mathcal{S} \mathcal{A}_l \mathcal{I}_1 \\ + \text{Sym}\{(\mathcal{I}_4^T + \kappa\mathcal{I}_1^T)\mathcal{K}^*(\mathcal{I}_2 - \mathcal{I}_{10})\} \end{aligned}$$

and other notations are defined in Theorem 1. The adaptive event-triggered sampled-data controller gain of (16) is

$$\mathcal{K} = \mathcal{S}^{-1}\mathcal{K}^*. \quad (51)$$

*Proof:* Let  $\mathcal{S}\mathcal{K} = \mathcal{K}^*$ . From Theorem 1, we find that (48)–(50) hold.

### C. Synchronization for Reaction–Diffusion Neural Networks With Event-Triggered Sampled-Data Control

When the event-triggered mechanism (13) is not adaptive, the threshold functions  $\delta(t_{0+\tau})$  and  $\delta(t_{\sigma_{k-1+\tau}})$  are reduced to a determined constant  $\delta^*$ . Following the similar proof of Theorem 2, we can obtain the following results.

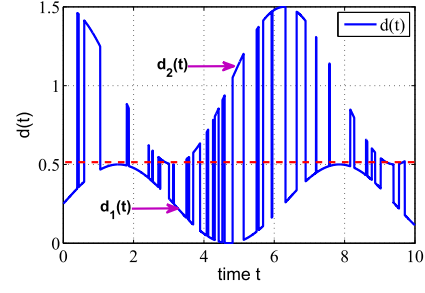


Fig. 1. Random time-varying delay  $d(t)$ .

*Theorem 3:* For given scalars  $0 \leq \gamma \leq 1$ ,  $\mu_i$  ( $i = 1, 2$ ),  $\tilde{h} > 0$ ,  $\delta^*$ , and  $\kappa$ , the response RDNN (7) is asymptotically synchronized to the drive RDNN (1) if there exist matrices  $\mathcal{P} > 0 \in \mathfrak{R}^{n \times n}$ ,  $\mathcal{Q}_i > 0 \in \mathfrak{R}^{2n \times 2n}$  ( $i = 1, 2$ ),  $\mathcal{T} > 0 \in \mathfrak{R}^{n \times n}$ ,  $\mathcal{R} > 0 \in \mathfrak{R}^{n \times n}$ , and  $\mathcal{B}_i > 0 \in \mathfrak{R}^{n \times n}$  ( $i = 1, 2$ ), diagonal matrices  $\mathcal{D}_i > 0 \in \mathfrak{R}^{n \times n}$  ( $i = 1, 2, 3$ ), and any matrices  $\mathcal{S} \in \mathfrak{R}^{n \times n}$ ,  $\mathcal{H}_1 \in \mathfrak{R}^{n \times 2n}$ ,  $\mathcal{H}_2 \in \mathfrak{R}^{n \times 3n}$ , and  $\mathcal{K}^* \in \mathfrak{R}^{n \times n}$  satisfying  $\mathcal{S}\mathcal{A}_l \geq 0$  and

$$\Xi^{**}(0; 0, 0) < 0 \quad (52)$$

$$\Xi^{**}(0; \tilde{h}, 0) < 0 \quad (53)$$

$$\begin{bmatrix} \Xi^{**}(0; \tilde{h}, \tilde{h}) & \sqrt{\tilde{h}}[\mathcal{I}_1^T, \mathcal{I}_2^T]\mathcal{H}_1^T & \sqrt{3\tilde{h}}[\mathcal{I}_1^T, \mathcal{I}_2^T, \mathcal{I}_5^T]\mathcal{H}_2^T \\ * & -\mathcal{R} & 0 \\ * & * & -\mathcal{R} \end{bmatrix} < 0 \quad (54)$$

where  $\Xi^{**}(\rho; h_{\sigma_{p-1+j}}, h(t)) = \sum_{i=2}^4 \Xi_i(\rho; h_{\sigma_{p-1+j}}, h(t)) + \Xi_1^*(\rho; h_{\sigma_{p-1+j}}, h(t)) + \Xi_5^*(\rho; h_{\sigma_{p-1+j}}, h(t))$  with

$$\begin{aligned} \Xi_1^*(\rho; h_{\sigma_{p-1+j}}, h(t)) \\ = \delta^*(\mathcal{I}_2 - \mathcal{I}_{10})^T \mathcal{B}_1 (\mathcal{I}_2 - \mathcal{I}_{10}) - \mathcal{I}_{10}^T \mathcal{B}_2 \mathcal{I}_{10} \end{aligned}$$

and other notations are defined in Theorems 1 and 2. Furthermore, the event-triggered sampled-data controller gain is given as

$$\mathcal{K} = \mathcal{S}^{-1}\mathcal{K}^*. \quad (55)$$

### D. Synchronization for Reaction–Diffusion Neural Networks With Sampled-Data Control

When the adaptive event-triggered mechanism (13) is not considered, the controller (15) is reduced to the following sampled-data controller:

$$\mathcal{U}(t, x) = \mathcal{K}\vartheta(t_k, x), \quad t_k \leq t < t_{k+1} \quad (56)$$

and the error system (17) is transformed into

$$\begin{aligned} \frac{\partial \vartheta(t, x)}{\partial t} = \sum_{l=1}^m \frac{\partial}{\partial x_l} \left( \mathcal{A}_l \frac{\partial \vartheta(t, x)}{\partial x_l} \right) - \mathcal{C}\vartheta(t, x) \\ + \mathcal{W}_1 f(\vartheta(t, x)) + \beta(t)\mathcal{W}_2 f(\vartheta(t - d_1(t), x)) \\ + (1 - \beta(t))\mathcal{W}_2 f(\vartheta(t - d_2(t), x)) \\ + \mathcal{K}\vartheta(t_k, x), \quad t \in [t_k, t_{k+1}), \quad x \in \Omega \end{aligned} \quad (57)$$

$$\vartheta(t, x) = 0, \quad (t, x) \in [\tilde{t}_0 - d_2, +\infty) \times \partial\Omega \quad (58)$$

$$\vartheta(s + \tilde{t}_0, x) = \psi(s, x) \in C([-d_2, 0] \times \Omega, \mathfrak{R}^n). \quad (59)$$

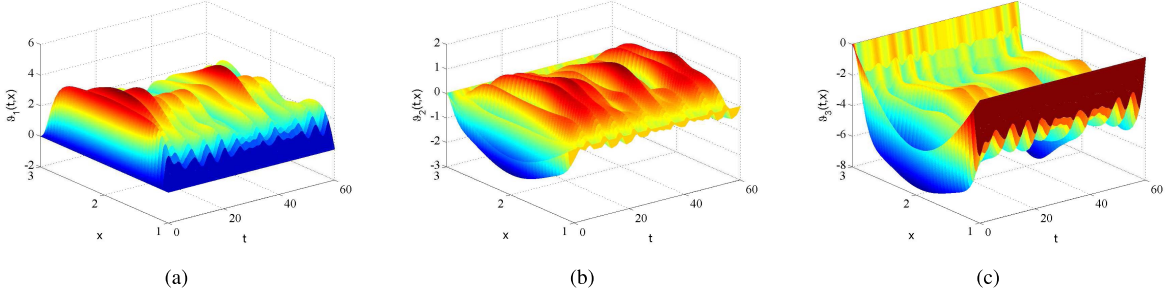


Fig. 2. Time-space behaviors of error system (10) with  $\mathcal{U}(t, x) = 0$ . (a)  $\vartheta_1(t, x)$  with  $\psi(s, x) = 0$ . (b)  $\vartheta_2(t, x)$  with  $\psi(s, x) = -1.5\Lambda(s, x)$ . (c)  $\vartheta_3(t, x)$  with  $\psi(s, x) = -5\Lambda(s, x)$ .

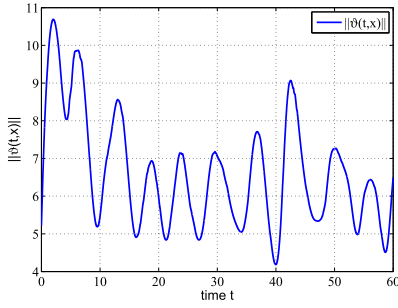


Fig. 3. Time responses of error signal  $\|\vartheta(t, x)\|_{L_2}$  with  $\mathcal{U}(t, x) = 0$ .

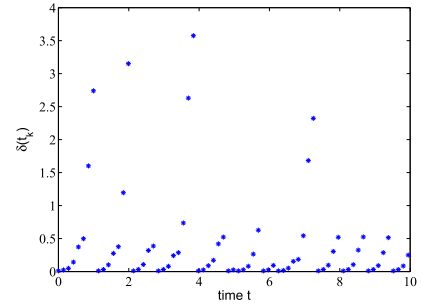


Fig. 4. Threshold function  $\delta(t_k)$  of the adaptive event-triggered communication mechanism (13).

Denote  $\hat{\mathcal{L}}_i = [0_{n,(i-1)n} \quad I_n \quad 0_{n,(9-i)n}]$ , ( $i = 1, \dots, 9$ ),  $\hat{h}(t) = t - t_k$ ,  $\hat{\xi}_3(t, x) = \begin{cases} (1/(t - t_k)) \int_{t_k}^t \vartheta(s, x) ds, & t \neq t_k, \\ \vartheta(t_k, x), & t = t_k, \end{cases}$  and  $\hat{\eta}(t, x) = \text{col}\{\vartheta(t, x), \vartheta(t - \hat{h}(t), x), f(\vartheta(t, x)), (\partial\vartheta(t, x)/\partial t), \hat{\xi}_3(t, x), \vartheta(t - d_1(t), x), \vartheta(t - d_2(t), x), f(\vartheta(t - d_1(t), x)), f(\vartheta(t - d_2(t), x))\}$ . Similar to the proof of Theorem 2, one can derive the following results.

*Theorem 4:* For given scalars  $0 \leq \gamma \leq 1$ ,  $\mu_i$  ( $i = 1, 2$ ),  $\tilde{h} > 0$ , and  $\kappa$ , the response RDNN (7) is asymptotically synchronized to the drive RDNN (1) if there exist matrices  $\mathcal{P} > 0 \in \mathfrak{R}^{n \times n}$ ,  $\mathcal{Q}_i > 0 \in \mathfrak{R}^{2n \times 2n}$  ( $i = 1, 2$ ),  $\mathcal{T} > 0 \in \mathfrak{R}^{n \times n}$ , and  $\mathcal{R} > 0 \in \mathfrak{R}^{n \times n}$ , diagonal matrices  $\mathcal{D}_i > 0 \in \mathfrak{R}^{n \times n}$  ( $i = 1, 2, 3$ ), and any matrices  $\mathcal{S} \in \mathfrak{R}^{n \times n}$ ,  $\mathcal{H}_1 \in \mathfrak{R}^{n \times 2n}$ ,  $\mathcal{H}_2 \in \mathfrak{R}^{n \times 3n}$ , and  $\mathcal{K}^* \in \mathfrak{R}^{n \times n}$  satisfying  $\mathcal{S}\mathcal{A}_i \geq 0$  and

$$\hat{\Xi}(0; 0, 0) < 0 \quad (60)$$

$$\hat{\Xi}(0; \tilde{h}, 0) < 0 \quad (61)$$

$$\begin{bmatrix} \hat{\Xi}(0; \tilde{h}, \tilde{h}) & \sqrt{\tilde{h}}[\hat{\mathcal{L}}_1^T, \hat{\mathcal{L}}_2^T]\mathcal{H}_1^T & \sqrt{3\tilde{h}}[\hat{\mathcal{L}}_1^T, \hat{\mathcal{L}}_2^T, \hat{\mathcal{L}}_5^T]\mathcal{H}_2^T \\ * & -\mathcal{R} & 0 \\ * & * & -\mathcal{R} \end{bmatrix} < 0 \quad (62)$$

where  $\hat{\Xi}(\rho; h_{\sigma_{p-1+j}}, h(t)) = \sum_{i=2}^5 \hat{\Xi}_i(\rho; h_k, \hat{h}(t))$  with

$$\begin{aligned} \hat{\Xi}_2(\rho; h_k, \hat{h}(t)) &= \text{Sym}\{(\hat{\mathcal{L}}_3 - \mathcal{F}^{-}\hat{\mathcal{L}}_1)^T \mathcal{D}_1 (\mathcal{F}^+ \hat{\mathcal{L}}_1 - \hat{\mathcal{L}}_3)\} \\ &\quad + \text{Sym}\{(\hat{\mathcal{L}}_8 - \mathcal{F}^{-}\hat{\mathcal{L}}_6)^T \mathcal{D}_2 (\mathcal{F}^+ \hat{\mathcal{L}}_6 - \hat{\mathcal{L}}_8)\} \\ &\quad + \text{Sym}\{(\hat{\mathcal{L}}_9 - \mathcal{F}^{-}\hat{\mathcal{L}}_7)^T \mathcal{D}_3 (\mathcal{F}^+ \hat{\mathcal{L}}_7 - \hat{\mathcal{L}}_9)\} \\ \hat{\Xi}_3(\rho; h_k, \hat{h}(t)) & \end{aligned}$$

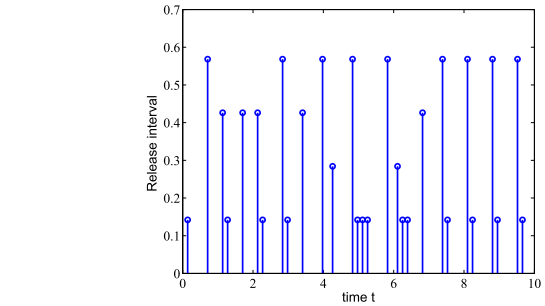


Fig. 5. Transmission instants and release intervals with  $\delta(t_k)$ .

$$\begin{aligned} &= \text{Sym}\{\hat{\mathcal{L}}_1^T \mathcal{P} \hat{\mathcal{L}}_4\} + \gamma [\hat{\mathcal{L}}_1^T, \hat{\mathcal{L}}_3^T] \mathcal{Q}_1 [\hat{\mathcal{L}}_1^T, \hat{\mathcal{L}}_3^T]^T \\ &\quad - \gamma (1 - \mu_1) [\hat{\mathcal{L}}_6^T, \hat{\mathcal{L}}_8^T] \mathcal{Q}_1 [\hat{\mathcal{L}}_6^T, \hat{\mathcal{L}}_8^T]^T \\ &\quad + (1 - \gamma) [\hat{\mathcal{L}}_1^T, \hat{\mathcal{L}}_3^T] \mathcal{Q}_2 [\hat{\mathcal{L}}_1^T, \hat{\mathcal{L}}_3^T]^T \\ &\quad - (1 - \gamma) (1 - \mu_2) [\hat{\mathcal{L}}_7^T, \hat{\mathcal{L}}_9^T] \mathcal{Q}_2 [\hat{\mathcal{L}}_7^T, \hat{\mathcal{L}}_9^T]^T \\ \hat{\Xi}_4(\rho; h_k, \hat{h}(t)) &= (h_k - \hat{h}(t)) \text{Sym}\{(\hat{\mathcal{L}}_1 - \hat{\mathcal{L}}_2)^T \mathcal{T} \hat{\mathcal{L}}_4\} \\ &\quad - (\hat{\mathcal{L}}_1 - \hat{\mathcal{L}}_2)^T \mathcal{T} (\hat{\mathcal{L}}_1 - \hat{\mathcal{L}}_2) + (h_k - \hat{h}(t)) \hat{\mathcal{L}}_4^T \mathcal{R} \hat{\mathcal{L}}_4 \\ &\quad - \text{Sym}\{(\hat{\mathcal{L}}_1 - \hat{\mathcal{L}}_2)^T \mathcal{H}_1 [\hat{\mathcal{L}}_1^T, \hat{\mathcal{L}}_2^T]^T\} \\ &\quad + \rho \hat{h}(t) [\hat{\mathcal{L}}_1^T, \hat{\mathcal{L}}_2^T] \mathcal{H}_1^T \mathcal{R}^{-1} \mathcal{H}_1 [\hat{\mathcal{L}}_1^T, \hat{\mathcal{L}}_2^T]^T \\ &\quad - 3 \text{Sym}\{(\hat{\mathcal{L}}_1 + \hat{\mathcal{L}}_2 - 2\hat{\mathcal{L}}_5)^T \mathcal{H}_2 [\hat{\mathcal{L}}_1^T, \hat{\mathcal{L}}_2^T, \hat{\mathcal{L}}_5^T]^T\} \\ &\quad + 3\rho \hat{h}(t) [\hat{\mathcal{L}}_1^T, \hat{\mathcal{L}}_2^T, \hat{\mathcal{L}}_5^T] \mathcal{H}_2^T \mathcal{R}^{-1} \mathcal{H}_2 [\hat{\mathcal{L}}_1^T, \hat{\mathcal{L}}_2^T, \hat{\mathcal{L}}_5^T]^T \\ \hat{\Xi}_5(\rho; h_k, \hat{h}(t)) & \end{aligned}$$

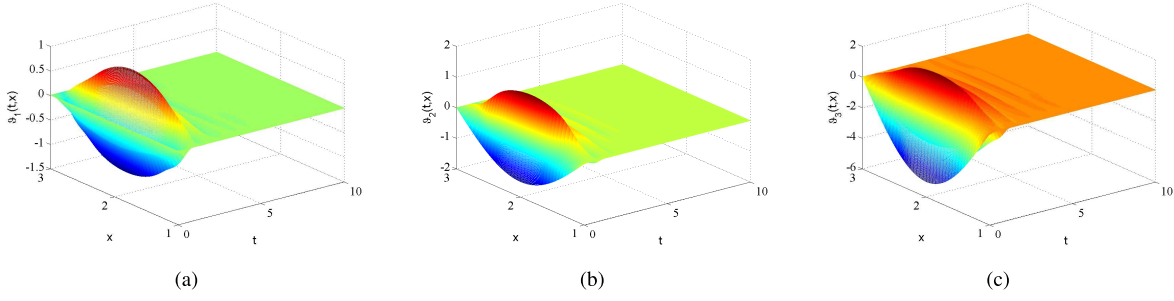


Fig. 6. Spatial behaviors of error signal  $\vartheta(t, x)$  with  $U(t, x)$ . (a)  $\vartheta_1(t, x)$ . (b)  $\vartheta_2(t, x)$ . (c)  $\vartheta_3(t, x)$ .

$$\begin{aligned}
&= \text{Sym}\{(\hat{\mathcal{I}}_4^T + \kappa \hat{\mathcal{I}}_1^T) \mathcal{S}(-\hat{\mathcal{I}}_4 - \mathcal{C} \hat{\mathcal{I}}_1 + \mathcal{W}_1 \hat{\mathcal{I}}_3 + \gamma \mathcal{W}_2 \hat{\mathcal{I}}_8 \\
&\quad + (1 - \gamma) \mathcal{W}_2 \hat{\mathcal{I}}_9)\} - 2\kappa \sum_{l=1}^m \frac{\pi^2}{(\bar{q}_l - \underline{q}_l)^2} \hat{\mathcal{I}}_1^T \mathcal{S} \mathcal{A}_l \hat{\mathcal{I}}_1 \\
&\quad + \text{Sym}\{(\hat{\mathcal{I}}_4^T + \kappa \hat{\mathcal{I}}_1^T) \mathcal{K}^* \hat{\mathcal{I}}_2\}.
\end{aligned}$$

Moreover, the sampled-data controller gain of (56) is

$$\mathcal{K} = \mathcal{S}^{-1} \mathcal{K}^*. \quad (63)$$

#### IV. NUMERICAL EXAMPLE

In this section, a numerical example is provided to verify the effectiveness and superiorities of the analysis results. In order to show how to obtain the maximum sampling interval (MSI)  $\tilde{h}$  and the corresponding solutions of matrices  $\mathcal{P}$ ,  $\mathcal{Q}_i$  ( $i = 1, 2$ ),  $\mathcal{T}$ , and others in Theorem 2 (Theorem 3 or 4), Algorithm 1 is given as follows.

*Algorithm 1: MSI Search and Feasible Solution Algorithm*

*Step 1:* For given  $0 \leq \gamma \leq 1$ ,  $\mu_i$  ( $i = 1, 2$ ),  $\tilde{h} > 0$ ,  $\delta_0$ , and  $\kappa$ , specify the ranges  $\tilde{h}$  with increments  $\Delta \tilde{h} > 0$ . Set  $\tilde{h} = \Delta \tilde{h}$ .

*Step 2:* Use MATLAB LMI Toolbox to solve LMIs in Theorem 2 with specified  $\tilde{h}$ .

*Step 3:* If there exists a feasible solution, then let  $\tilde{h} = \tilde{h} + \Delta \tilde{h}$ , and go to Step 2. Otherwise, go to Step 4.

*Step 4:* If  $\tilde{h} = \Delta \tilde{h}$ , output “No feasible solution satisfying Theorem 2”. Then reselect values of  $\delta_0$ ,  $\kappa$ , go to Step 1. Otherwise, go to Step 5.

*Step 5:* Output  $\tilde{h} = \tilde{h} - \Delta \tilde{h}$ , which is the MSI. With the output MSI  $\tilde{h}$ , and using MATLAB LMI Toolbox to solve the LMIs in Theorem 2, we get the corresponding solutions of matrices  $\mathcal{P}$ ,  $\mathcal{Q}_i$  ( $i = 1, 2$ ),  $\mathcal{T}$ , and others.

Consider the 3-D RDNN (1) with the following parameters:

$$\begin{aligned}
\mathcal{A}_1 &= \text{diag}\{0.01, 0.01, 0.01\}, \quad \mathcal{C} = I_3 \\
\mathcal{W}_1 &= \begin{bmatrix} 1.2 & -1.6 & 0 \\ 1.24 & 1 & 0.9 \\ 0 & 2.2 & 1.5 \end{bmatrix} \\
\mathcal{W}_2 &= \begin{bmatrix} 0.1 & -0.5 & 0 \\ 0.24 & 0.21 & 0.2 \\ 0 & 1.2 & 0.6 \end{bmatrix} \\
\Omega &= \{x | 1 \leq x \leq 3\}, \quad J = 0 \\
g_i(\varpi_i(t, x)) &= \frac{1}{2}(|\varpi_i(t, x) + 1| - |\varpi_i(t, x) - 1|)
\end{aligned}$$

where  $i = 1, 2, 3$ . It is obvious that  $g_i(\varpi_i(t, x))$  satisfies Assumption 1 with  $l_1^- = l_2^- = l_3^- = 0$  and  $l_1^+ = l_2^+ = l_3^+ = 1$ .

Take  $\gamma = 0.7$ ,  $d_1(t) = 0.25 + 0.25 \sin(t)$ , and  $d_2(t) = 1 + 0.5 \cos(t)$ , from which one obtains  $\mu_1 = 0.25$ ,  $\mu_2 = 0.5$ , and  $d_1 = 0.5$ . Similar to [20] and [48], assume the random time-varying delay  $d(t)$  be a Markov process with transition rate matrix  $(1/\mathcal{T}) \times \begin{bmatrix} \gamma - 1 & 1 - \gamma \\ \gamma & -\gamma \end{bmatrix}$ , where the updated period  $\mathcal{T} = 0.1$ . The time responses of random time-varying delay  $d(t)$  are displayed in Fig. 1. From Fig. 1, one finds that the random time-varying delay  $d(t)$  switches between  $d_1(t)$  and  $d_2(t)$ .

Choose the initial conditions as

$$\begin{aligned}
\psi_1(s, x) &: \text{col}\{-\Lambda(s, x), 0.5\Lambda(s, x), \Lambda(s, x)\} \\
\psi_2(s, x) &: \text{col}\{-\Lambda(s, x), -\Lambda(s, x), -4\Lambda(s, x)\}
\end{aligned}$$

where  $\Lambda(s, x) = \cos(((2x - 4)\pi)/4)$ . Then, when  $U(t, x) = 0$ , the time-space behaviors of error system (10) are shown in Fig. 2, and the time responses of error signal  $\|\vartheta(t, x)\|_{L_2}$  are plotted in Fig. 3, from which we can find that the synchronization of RDNNs (1) and (7) cannot be achieved if there is no control input.

Now, we show the effectiveness and advantages of Theorem 2. Take  $\delta_0 = 0.01$ ,  $\theta = 3$ ,  $\gamma = 0.7$ ,  $\kappa = 3$ ,  $\mu_1 = 0.25$ ,  $\mu_2 = 0.5$ , and set  $9\delta_0 \mathcal{B}_1 > \mathcal{B}_2$ . By Algorithm 1, we find the MSI  $\tilde{h} = 0.1421$  and obtain the solutions of matrices as (to save space, we only list some of the obtained matrices) the matrices can be derived, as shown at the bottom of next page. Then, from (51), the adaptive event-triggered sampled-data controller gain is

$$\mathcal{K} = \begin{bmatrix} -1.8999 & 0.0999 & 1.1411 \\ -0.8020 & -3.3004 & -0.7980 \\ 0.9529 & -2.3492 & -3.6566 \end{bmatrix}.$$

With the abovementioned parameters, by the adaptive event-triggered communication mechanism (13), the threshold function  $\delta(t_k)$  is displayed in Fig. 4, which shows that  $\delta(t_k)$  can be dynamically adjusted based on the current sampled and latest transmitted signals. The transmission instants and release intervals are plotted in Fig. 5. From Fig. 5, we find that, when  $t = 10$ , the number of transmitted signals (NTSs) is 29. Fig. 6 represents the controlled spatial behaviors of error signal  $\vartheta(t, x)$ , and the trajectories of the controlled signal  $\|\vartheta(t, x)\|_{L_2}$  are displayed in Fig. 7. From Figs. 6 and 7, we find that the synchronization of RDNNs (1) and (7)

TABLE I  
NTSS AND APs FOR VARIOUS SCHEMES

Scheme	NTSs	APs	Improvement rates (%)
Theorem 2	29	0.3448	
Theorem 3	42	0.2380	44.87%
Theorem 4	70	0.1428	141.45%

TABLE II  
NTSS FOR VARIOUS  $\theta$ 's

$\theta$	0.1	0.3	0.5	1.0	2.0	3.0
NTS	38	37	32	26	28	29

is realized under the adaptive event-triggered sampled-data controller  $\mathcal{U}(t, x)$  in (15), where the adaptive event-triggered sampled-data controller  $\mathcal{U}(t, x)$  is shown in Fig. 8.

By various schemes, the number of NTSs and average periods (APs) is listed in Table I. From Table I, one finds that, by the adaptive event-triggered scheme in Theorem 2, the event-triggered scheme in Theorem 3, and the sampled-data control scheme in Theorem 4, the NTSs are 29, 42, and 70, and the APs are 0.3448, 0.2380, and 0.1428, respectively. The AP of the adaptive event-triggered scheme in Theorem 2 improves 44.87% and 141.45% than that of

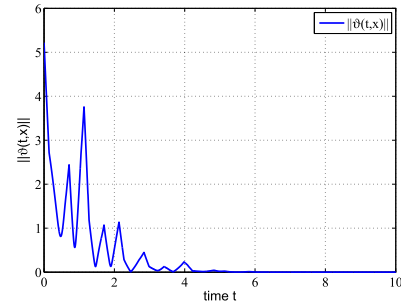


Fig. 7. Trajectories of the error signal  $\|\vartheta(t, x)\|_{L^2}$  with the adaptive event-triggered sampled-data controller  $\mathcal{U}(t, x)$ .

Theorems 3 and 4, respectively. Thus, compared with the schemes of Theorems 3 and 4, the adaptive event-triggered scheme in Theorem 2 can effectively reduce the transmission signals to save the communication resources. Meanwhile, by using MATLAB 8.0.0.783 (R2012b) running on a PC with 2.50-GHz Intel Core i7 CPU, 8-GB RAM, and Windows 10 64-bit Ultimate, the calculation costs of the adaptive event-triggered scheme in Theorem 2, the event-triggered scheme in Theorem 3, and the sampled-data control scheme in Theorem 4 are 15.254834, 12.020567, and 11.281892 s,

$$\begin{aligned}
 \mathcal{P} &= \begin{bmatrix} 2.0576 & -0.7085 & 0.7470 \\ -0.7085 & 1.7663 & -0.3834 \\ 0.7470 & -0.3834 & 0.7375 \end{bmatrix} \\
 \mathcal{Q}_1 &= \begin{bmatrix} 2.6257 & -0.8719 & 0.5472 & -1.6348 & 0.9302 & 0.0430 \\ -0.8719 & 1.7606 & -0.9880 & -0.0913 & -1.5033 & 0.7556 \\ 0.5472 & -0.9880 & 0.6240 & 0.2623 & 0.8968 & -0.4241 \\ -1.6348 & -0.0913 & 0.2623 & 2.3361 & 0.0075 & -0.4813 \\ 0.9302 & -1.5033 & 0.8968 & 0.0075 & 3.3123 & -0.8309 \\ 0.0430 & 0.7556 & -0.4241 & -0.4813 & -0.8309 & 0.8681 \end{bmatrix} \\
 \mathcal{Q}_2 &= \begin{bmatrix} 5.2972 & -1.6710 & 1.0817 & -3.3399 & 1.7325 & 0.1344 \\ -1.6710 & 3.5694 & -1.9986 & -0.2521 & -3.0165 & 1.4823 \\ 1.0817 & -1.9986 & 1.2748 & 0.5970 & 1.7254 & -0.8616 \\ -3.3399 & -0.2521 & 0.5970 & 4.9238 & -0.0552 & -1.0963 \\ 1.7325 & -3.0165 & 1.7254 & -0.0552 & 6.0008 & -1.8674 \\ 0.1344 & 1.4823 & -0.8616 & -1.0963 & -1.8674 & 1.5572 \end{bmatrix} \\
 \mathcal{T} &= \begin{bmatrix} 3.3068 & -1.0311 & 1.2505 \\ -1.0311 & 3.3526 & -0.6795 \\ 1.2505 & -0.6795 & 1.3331 \end{bmatrix} \\
 \mathcal{S} &= \begin{bmatrix} 0.6559 & -0.2241 & 0.3114 \\ -0.2148 & 0.4708 & -0.1472 \\ 0.2439 & -0.1400 & 0.2236 \end{bmatrix} \\
 \mathcal{K}^* &= \begin{bmatrix} -0.7696 & 0.0737 & -0.2113 \\ -0.1097 & -1.2296 & -0.0827 \\ -0.1381 & -0.0391 & -0.4277 \end{bmatrix} \\
 \mathcal{B}_1 &= \begin{bmatrix} 64.3921 & 17.7032 & 8.1665 \\ 17.7032 & 155.2993 & 43.6707 \\ 8.1665 & 43.6707 & 56.9334 \end{bmatrix} \\
 \mathcal{B}_2 &= \begin{bmatrix} 5.3630 & 1.6145 & 0.6230 \\ 1.6145 & 13.6247 & 4.0925 \\ 0.6230 & 4.0925 & 5.0247 \end{bmatrix}
 \end{aligned}$$

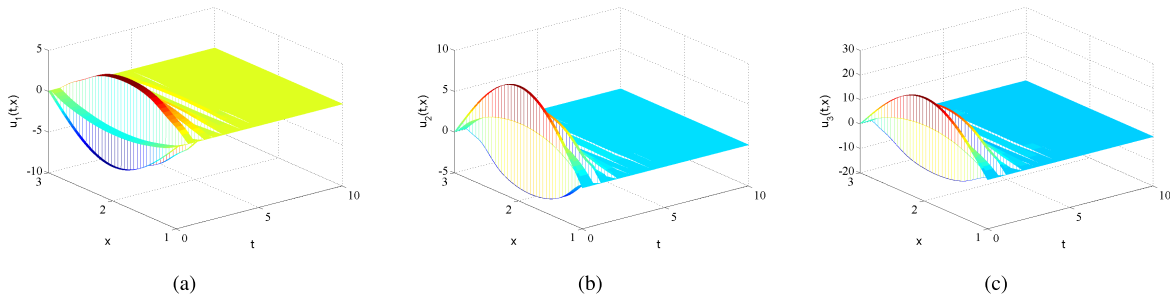


Fig. 8. Spatial behaviors of the adaptive event-triggered sampled-data controller  $\mathcal{U}(t, x)$  in (15). (a)  $u_1(t, x)$ . (b)  $u_2(t, x)$ . (c)  $u_3(t, x)$ .

respectively. Compared with the control schemes in Theorems 3 and 4, the control scheme in Theorem 2 increases the calculation cost since its threshold function is time-varying and adaptive. Furthermore, for different values of  $\theta$ , the NTSS of the adaptive event-triggered mechanism (13) are given in Table II, from which we find that the values of  $\theta$  have some impact on the NTSSs.

## V. CONCLUSION

In this article, we have studied the synchronization of RDNNs with random time-varying delays. By designing an adaptive aperiodic ETSDC scheme and introducing an appropriate LKF, we have established some new synchronization criteria for RDNNs. Different from the existing ETSDC methods with constant thresholds, our method can be adaptively adjusted according to the current sampled and latest transmitted signals. In comparison with the existing control methods, our method can effectively save the communication resources for RDNNs. Taking the influence of uncertain factors, the random time-varying delays have been considered for RDNNs, which makes the obtained results more applicable. In the end, we have presented some simulations to show the superiorities of the adaptive ETSDC mechanism and the effectiveness of the obtained results.

## REFERENCES

- [1] A. Cocheci and R. Unbehauen, *Neural Networks for Optimization and Signal Processing*. Hoboken, NJ, USA: Wiley, 1993.
- [2] Z. Zhou and C. Gao, *Neural Network With Applications*. Beijing, China: Tsinghua Univ. Press, 2004.
- [3] J. H. Park, H. Shen, X. H. Chang, and T. H. Lee, *Recent Advances in Control and Filtering of Dynamic Systems with Constrained Signals*. Cham, Switzerland: Springer, 2018.
- [4] L. O. Chua and L. Yang, "Cellular neural networks: Applications," *IEEE Trans. Circuits Syst.*, vol. 35, no. 10, pp. 1273–1290, Oct. 1988.
- [5] R. Zhang, D. Zeng, J. H. Park, Y. Liu, and S. Zhong, "Quantized sampled-data control for synchronization of inertial neural networks with heterogeneous time-varying delays," *IEEE Trans. Neural Netw. Learn. Syst.*, vol. 29, no. 12, pp. 6385–6395, Dec. 2018.
- [6] W. Xie, H. Zhu, J. Cheng, S. Zhong, and K. Shi, "Finite-time asynchronous  $H_\infty$  resilient filtering for switched delayed neural networks with memory unideal measurement," *Inf. Sci.*, vol. 487, pp. 156–175, Jun. 2019.
- [7] J. Xiao and S. Zhong, "Extended dissipative conditions for memristive neural networks with multiple time delays," *Appl. Math. Comput.*, vol. 323, pp. 145–163, Apr. 2018.
- [8] C. Prieur and E. Trélat, "Feedback stabilization of a 1-D linear reaction-diffusion equation with delay boundary control," *IEEE Trans. Autom. Control*, vol. 64, no. 4, pp. 1415–1425, Apr. 2019.
- [9] Z.-P. Wang, H.-N. Wu, J.-L. Wang, and H.-X. Li, "Quantized sampled-data synchronization of delayed reaction-diffusion neural networks under spatially point measurements," *IEEE Trans. Cybern.*, early access, Jan. 9, 2020, doi: 10.1109/TCYB.2019.2960094.
- [10] P. Arena, L. Fortuna, and M. Branciforte, "Reaction-diffusion CNN algorithms to generate and control artificial locomotion," *IEEE Trans. Circuits Syst. I, Fundam. Theory Appl.*, vol. 46, no. 2, pp. 253–260, Feb. 1999.
- [11] W.-H. Chen, S. Luo, and W. Xing Zheng, "Impulsive synchronization of reaction-diffusion neural networks with mixed delays and its application to image encryption," *IEEE Trans. Neural Netw. Learn. Syst.*, vol. 27, no. 12, pp. 2696–2710, Dec. 2016.
- [12] J. D. Murray, *Mathematical Biology*. New York, NY, USA: Springer-Verlag, 1989.
- [13] J.-L. Wang, Z. Qin, H.-N. Wu, and T. Huang, "Passivity and synchronization of coupled uncertain reaction-diffusion neural networks with multiple time delays," *IEEE Trans. Neural Netw. Learn. Syst.*, vol. 30, no. 8, pp. 2434–2448, Aug. 2019.
- [14] Y. Sheng, H. Zhang, and Z. Zeng, "Stability and robust stability of stochastic reaction-diffusion neural networks with infinite discrete and distributed delays," *IEEE Trans. Syst., Man, Cybern. Syst.*, vol. 50, no. 5, pp. 1721–1732, May 2020.
- [15] H. Zhang, N. R. Pal, Y. Sheng, and Z. Zeng, "Distributed adaptive tracking synchronization for coupled reaction-diffusion neural network," *IEEE Trans. Neural Netw. Learn. Syst.*, vol. 30, no. 5, pp. 1462–1475, May 2019.
- [16] L. M. Pecora and T. L. Carroll, "Synchronization in chaotic systems," *Phys. Rev. Lett.*, vol. 64, no. 8, pp. 821–824, 1990.
- [17] H. Shen, T. Wang, J. Cao, G. Lu, Y. Song, and T. Huang, "Nonfragile dissipative synchronization for Markovian memristive neural networks: A gain-scheduled control scheme," *IEEE Trans. Neural Netw. Learn. Syst.*, vol. 30, no. 6, pp. 1841–1853, Jun. 2019.
- [18] V. Milanović and M. E. Zaghoul, "Synchronization of chaotic neural networks and applications to communications," *Int. J. Bifurcation Chaos*, vol. 6, no. 12, pp. 2571–2585, Dec. 1996.
- [19] J. H. Park, T. H. Lee, Y. Liu, and J. Chen, *Dynamic Systems With Time Delays: Stability and Control*. Singapore: Springer, 2019, doi: 10.1007/978-981-13-9254-2.
- [20] A. P. Isle, "Stability of systems with nonlinear feedback through randomly time-varying delays," *IEEE Trans. Autom. Control*, vol. 20, no. 1, pp. 67–75, Feb. 1975.
- [21] A. Ray, "Output feedback control under randomly varying distributed delays," *J. Guid., Control, Dyn.*, vol. 17, no. 4, pp. 701–711, Jul. 1994.
- [22] C. Peng and J. Zhang, "Delay-distribution-dependent load frequency control of power systems with probabilistic interval delays," *IEEE Trans. Power Syst.*, vol. 31, no. 4, pp. 3309–3317, Jul. 2016.
- [23] D. Yue, Y. Zhang, E. Tian, and C. Peng, "Delay-distribution-dependent exponential stability criteria for discrete-time recurrent neural networks with stochastic delay," *IEEE Trans. Neural Netw.*, vol. 19, no. 7, pp. 1299–1306, Jul. 2008.
- [24] R. Sakthivel, S. Selvi, K. Mathiyalagan, and P. Shi, "Reliable mixed  $H_\infty$  and passivity-based control for fuzzy Markovian switching systems with probabilistic time delays and actuator failures," *IEEE Trans. Cybern.*, vol. 45, no. 12, pp. 2720–2731, Dec. 2015.

- [25] H. Bao, J. H. Park, and J. Cao, "Exponential synchronization of coupled stochastic memristor-based neural networks with time-varying probabilistic delay coupling and impulsive delay," *IEEE Trans. Neural Netw. Learn. Syst.*, vol. 27, no. 1, pp. 190–201, Jan. 2016.
- [26] Y. Sheng and Z. Zeng, "Impulsive synchronization of stochastic reaction–diffusion neural networks with mixed time delays," *Neural Netw.*, vol. 103, pp. 83–93, Jul. 2018.
- [27] X. Liu, K. Zhang, and W.-C. Xie, "Pinning impulsive synchronization of reaction–diffusion neural networks with time-varying delays," *IEEE Trans. Neural Netw. Learn. Syst.*, vol. 28, no. 5, pp. 1055–1067, May 2017.
- [28] Y. Wu, L. Liu, J. Hu, and G. Feng, "Adaptive antisynchronization of multilayer reaction–diffusion neural networks," *IEEE Trans. Neural Netw. Learn. Syst.*, vol. 29, no. 4, pp. 807–818, Apr. 2018.
- [29] X. Yang, Q. Song, J. Cao, and J. Lu, "Synchronization of coupled Markovian reaction–diffusion neural networks with proportional delays via quantized control," *IEEE Trans. Neural Netw. Learn. Syst.*, vol. 30, no. 3, pp. 951–958, Mar. 2019.
- [30] X. Wang, J. H. Park, S. Zhong, and H. Yang, "A switched operation approach to sampled-data control stabilization of fuzzy memristive neural networks with time-varying delay," *IEEE Trans. Neural Netw. Learn. Syst.*, vol. 31, no. 3, pp. 891–900, Mar. 2020.
- [31] Y. Liu, B.-Z. Guo, J. H. Park, and S.-M. Lee, "Nonfragile exponential synchronization of delayed complex dynamical networks with memory sampled-data control," *IEEE Trans. Neural Netw. Learn. Syst.*, vol. 29, no. 1, pp. 118–128, Jan. 2018.
- [32] E. Fridman, "A refined input delay approach to sampled-data control," *Automatica*, vol. 46, no. 2, pp. 421–427, Feb. 2010.
- [33] B. Lu, H. Jiang, C. Hu, and A. Abdurahman, "Synchronization of hybrid coupled reaction–diffusion neural networks with time delays via generalized intermittent control with spacial sampled-data," *Neural Netw.*, vol. 105, pp. 75–87, Sep. 2018.
- [34] R. Zhang, D. Zeng, J. H. Park, H.-K. Lam, and X. Xie, "Fuzzy sampled-data control for synchronization of T-S fuzzy reaction-diffusion neural networks with additive time-varying delays," *IEEE Trans. Cybern.*, early access, Jun. 10, 2020, doi: [10.1109/TCYB.2020.2996619](https://doi.org/10.1109/TCYB.2020.2996619).
- [35] S. Chen, C.-C. Lim, P. Shi, and Z. Lu, "Synchronization control for reaction–diffusion FitzHugh–Nagumo systems with spatial sampled-data," *Automatica*, vol. 93, pp. 352–362, Jul. 2018.
- [36] D. Yue, E. Tian, and Q.-L. Han, "A delay system method for designing event-triggered controllers of networked control systems," *IEEE Trans. Autom. Control*, vol. 58, no. 2, pp. 475–481, Feb. 2013.
- [37] C. Peng and Q.-L. Han, "A novel event-triggered transmission scheme and  $L_2$  control co-design for sampled-data control systems," *IEEE Trans. Autom. Control*, vol. 58, no. 10, pp. 2620–2626, Oct. 2013.
- [38] C. Peng, M. Wu, X. Xie, and Y.-L. Wang, "Event-triggered predictive control for networked nonlinear systems with imperfect premise matching," *IEEE Trans. Fuzzy Syst.*, vol. 26, no. 5, pp. 2797–2806, Oct. 2018.
- [39] H. Shen, F. Li, H. Yan, H. R. Karimi, and H.-K. Lam, "Finite-time event-triggered  $H_\infty$  control for T-S fuzzy Markov jump systems," *IEEE Trans. Fuzzy Syst.*, vol. 26, no. 5, pp. 3122–3135, Oct. 2018.
- [40] R. Yang, H. Zhang, G. Feng, H. Yan, and Z. Wang, "Robust cooperative output regulation of multi-agent systems via adaptive event-triggered control," *Automatica*, vol. 102, pp. 129–136, Apr. 2019.
- [41] Z. Gu, D. Yue, and E. Tian, "On designing of an adaptive event-triggered communication scheme for nonlinear networked interconnected control systems," *Inf. Sci.*, vol. 422, pp. 257–270, Jan. 2018.
- [42] Z. Gu, P. Shi, D. Yue, and Z. Ding, "Decentralized adaptive event-triggered  $H_\infty$  filtering for a class of networked nonlinear interconnected systems," *IEEE Trans. Cybern.*, vol. 49, no. 5, pp. 1570–1579, May 2019.
- [43] C. Peng, J. Zhang, and H. Yan, "Adaptive event-triggering  $H_\infty$  load frequency control for network-based power systems," *IEEE Trans. Ind. Electron.*, vol. 65, no. 2, pp. 1685–1694, Feb. 2018.
- [44] A. Seuret and F. Gouaisbaud, "Wirtinger-based integral inequality: Application to time-delay systems," *Automatica*, vol. 49, no. 9, pp. 2860–2866, Sep. 2013.
- [45] D. Zeng, R. Zhang, J. H. Park, Z. Pu, and Y. Liu, "Pinning synchronization of directed coupled reaction-diffusion neural networks with sampled-data communications," *IEEE Trans. Neural Netw. Learn. Syst.*, vol. 31, no. 6, pp. 2092–2103, Jun. 2020, doi: [10.1109/TNNLS.2019.2928039](https://doi.org/10.1109/TNNLS.2019.2928039).
- [46] X. Liang, L. Wang, Y. Wang, and R. Wang, "Dynamical behavior of delayed reaction–diffusion Hopfield neural networks driven by infinite dimensional Wiener processes," *IEEE Trans. Neural Netw. Learn. Syst.*, vol. 27, no. 9, pp. 1816–1826, Sep. 2016.

- [47] D. Yue, E. Tian, Y. Zhang, and C. Peng, "Delay-distribution-dependent robust stability of uncertain systems with time-varying delay," *Int. J. Robust Nonlinear Control*, vol. 19, no. 4, pp. 377–393, Mar. 2009.
- [48] N. Pang, Y. Luo, and Y. Zhu, "A novel model for linear dynamic system with random delays," *Automatica*, vol. 99, pp. 346–351, Jan. 2019.



**Ruimei Zhang** received the Ph.D. degree in applied mathematics from the School of Mathematical Sciences, University of Electronic Science and Technology of China, Chengdu, China, in 2019.

From 2017 to 2018, she was a Visiting Scholar with the Department of Applied Mathematics, University of Waterloo, Waterloo, ON, Canada. From 2018 to 2019, she was a Visiting Scholar with the Department of Electrical Engineering, Yeungnam University, Gyeongsan, South Korea. In 2020, she joined the College of Cybersecurity, Sichuan Uni-

versity, Chengdu, where she is currently a Distinguished Associate Research Fellow. Her current research interests include memristive neural networks, reaction–diffusion neural networks, and synchronization or stability of control systems with delay.



**Deqiang Zeng** was born in Yibin, China. He received the B.S. degree in mathematics and applied mathematics from Sichuan Normal University, Chengdu, China, in 2002, where he is currently pursuing the Ph.D. degree.

He is a Professor with the College of Mathematics and Information Science, Neijiang Normal University, Neijiang, China. His current research interests include sampled-data control, synchronization, reaction–diffusion systems, stochastic Markov jump, and complex network systems.



**Ju H. Park** (Senior Member, IEEE) received the Ph.D. degree in electronics and electrical engineering from the Pohang University of Science and Technology (POSTECH), Pohang, South Korea, in 1997.

From May 1997 to February 2000, he was a Research Associate with the Engineering Research Center–Automation Research Center, POSTECH. He joined Yeungnam University, Gyeongsan, South Korea, in March 2000, where he is currently the Chuma Chair Professor. He is a coauthor of the monographs *Recent Advances in Control and Filtering of Dynamic Systems with Constrained Signals* (New York, NY, USA: Springer-Nature, 2018) and *Dynamic Systems With Time Delays: Stability and Control* (New York, NY, USA: Springer-Nature, 2019) and is an Editor of an edited volume *Recent Advances in Control Problems of Dynamical Systems and Networks* (New York: Springer-Nature, 2020). His research interests include robust control and filtering, neural/complex networks, fuzzy systems, multiagent systems, and chaotic systems. He has published a number of articles in these areas.

Prof. Park is a fellow of the Korean Academy of Science and Technology (KAST). Since 2015, he has been a recipient of the Highly Cited Researcher Award by Clarivate Analytics (formerly, Thomson Reuters) and listed in three fields, engineering, computer sciences, and mathematics, in 2019. He also serves as an Editor of *International Journal of Control, Automation and Systems*. He is also a Subject Editor/Advisory Editor/Associate Editor/Editorial Board Member of several international journals, including *IET Control Theory & Applications*, *Applied Mathematics and Computation*, *Journal of The Franklin Institute*, *Nonlinear Dynamics*, *Engineering Reports*, *Cogent Engineering*, the IEEE TRANSACTIONS ON FUZZY SYSTEMS, the IEEE TRANSACTIONS ON NEURAL NETWORKS AND LEARNING SYSTEMS, and the IEEE TRANSACTIONS ON CYBERNETICS.



**Yajuan Liu** received the B.S. degree in mathematics and applied mathematics from Shanxi Normal University, Linfen, China, in 2010, the M.S. degree in applied mathematics from the University of Science and Technology Beijing, Beijing, China, in 2012, and the Ph.D. degree from the Division of Electronic Engineering, Daegu University, Daegu, South Korea, in 2015.

From 2015 to 2018, she was a Post-Doctoral Research Fellow with the Department of Electrical Engineering, Yeungnam University, Gyeongsan, South Korea. She is currently an Associate Professor with the School of Control and Computer Engineering, North China Electric Power University, Beijing. Her research focus is on control of dynamic systems, including neural networks and complex systems.



**Xiangpeng Xie** (Member, IEEE) received the B.S. and Ph.D. degrees in engineering from Northeastern University, Shenyang, China, in 2004 and 2010, respectively.

From 2010 to 2014, he was a Senior Engineer with the Metallurgical Corporation of China Ltd., Beijing, China. He is currently a Professor with the Institute of Advanced Technology, Nanjing University of Posts and Telecommunications, Nanjing, China. His research interests include fuzzy modeling and control synthesis, state estimations, optimization in process industries, and intelligent optimization algorithms.

Prof. Xie serves as an Associate Editor for the *International Journal of Control, Automation, and Systems* and the *International Journal of Fuzzy Systems*.